

Independent-Particle Model of the Nucleus. III. The Calcium Isotopes*

CARL LEVINSON† AND KENNETH W. FORD‡
Indiana University, Bloomington, Indiana

(Received May 31, 1955)

The isotopes of calcium of mass number 41, 42, and 43 are analyzed using the methods given in papers I and II of this series. It is found that the experimental data on Ca^{41} and Ca^{42} is sufficient to predict the low-lying odd-parity levels of Ca^{43} as well as the magnetic moment. Detailed agreement between theory and experiment is obtained for the levels of Ca^{43} of spin and parity $7/2^-$, $5/2^-$, $3/2^-$, and $9/2^-$ and the experimental Schmidt line magnetic moment deviation of 0.595 nm is in agreement with a predicted deviation of 0.60 nm. The relative importance of particle forces and surface forces due to collective motion is investigated and it is concluded that for the isotopes investigated the surface forces are so weak as to have a negligible effect on the level spacings. As a measure of the upper limit of the strength of the surface forces the magnitude of $\hbar\omega$ (the surfon energy) is set at $\gtrsim 15$ Mev. An effective two-particle interaction potential is derived which differs to some extent from the two-particle scattering potential in that it has a longer range and is more shallow.

INTRODUCTION

IN this paper, we shall apply the methods outlined in papers I and II² to the nuclei Ca^{41} , Ca^{42} , and Ca^{43} . The empirically determined single-particle levels of Ca^{41} determine the zero-order scheme and define the relevant configurations in Ca^{42} and Ca^{43} and their energy spacings. The experimental level scheme of Ca^{42} then serves to determine the necessary information about the two-body interaction which allows us to calculate the level scheme, wave functions, and magnetic moment of Ca^{43} . In order to apply these methods it is essential that the low-lying "single-particle" levels (i.e., $f_{7/2}$, $p_{3/2}$, $f_{5/2}$, $p_{1/2}$, $g_{9/2}$) of Ca^{41} be well represented by independent-particle wave functions. If the Ca^{40} core were truly inert and rigorously replaceable by a single-particle potential well, then the method described above would be exact. As a matter of fact, Ca^{40} has its first excited state at 3.75 Mev and core excitation states in Ca^{41} seem to appear at 2.6 Mev and higher. Since empirical information concerning the levels of Ca^{41} and Ca^{42} is used it is clear that some corrections due to core excitations are automatically included. For example, all corrections to the level spacing of Ca^{42} which can be interpreted as corrections due to core excitation that should be present for one of the extra core particles alone are already included since the empirical levels of Ca^{41} are used in setting up the problem. Similarly a large class of core excitation corrections to the level scheme of Ca^{43} are included since the potential has been adjusted to the empirical levels of Ca^{41} and Ca^{42} . This problem has been investigated in detail by Brueckner, Eden, and Francis³ who find that in adjusting a two-

body interaction to the empirical levels of Ca^{42} the core excitation corrections are automatically included for this problem. In the case of Ca^{43} , the approach again includes most of the corrections and one can expect a high degree of accuracy in the final results. If core excitation corrections are indeed small, then the empirically derived matrix elements for the Ca^{42} problem should be derivable from a two-body potential which fits the nucleon-nucleon scattering data. If, on the other hand, these corrections are appreciable then the effective potential may be somewhat different from the scattering one.

The only easy way to take explicit account of core excitations is through the collective model of coupling to nuclear surface oscillations. We have attempted to include such coupling in the calculations as a perturbation to the more detailed shell model treatment, but with the result that the closest agreement to experiment is obtained with zero additional surface coupling. This does not rule out, of course, that effects of a deformable core on the energies are already included in the semi-empirical approach outlined above. Diagonal contributions of weak surface coupling and of direct particle interaction are in fact indistinguishable in this approach. Off-diagonal contributions (configuration mixing) are, however, somewhat different.

I. LEVELS OF Ca^{41}

Ca^{41} consists of a doubly magic Ca^{40} core and a single neutron. According to the shell model, this neutron has an $f_{7/2}$ ground state and excited states of $p_{3/2}$, $f_{5/2}$, $p_{1/2}$, $g_{9/2}$, $d_{5/2}$ and $g_{7/2}$ in that order.⁴ The first seven excited states of Ca^{41} are according to Braams at 1.947, 2.015, 2.469, 2.582, 2.611, 2.675, and 2.890 ± 0.010 Mev.⁵ The ground state of Ca^{41} has an experimental shell model assignment of $f_{7/2}$.⁵ The 1.95- and 2.47-Mev levels have experimental spin and orbital angular momentum

* Supported in part by a grant from the National Science Foundation.

† Now at Palmer Physical Laboratory, Princeton University, Princeton, New Jersey.

‡ Now on leave at Max Planck Institut für Physik, Göttingen, Germany.

¹ C. A. Levinson and K. W. Ford, Phys. Rev. **99**, 792 (1955). Referred to as I in the balance of this paper.

² K. W. Ford and C. A. Levinson, preceding paper [Phys. Rev. **100**, 1 (1955)]. Referred to as II in the balance of this paper.

³ Brueckner, Eden, and Francis, Phys. Rev. (to be published).

⁴ P. F. A. Klinkenberg, Revs. Modern Phys. **24**, 63 (1952).

⁵ P. M. Endt and J. C. Kluver, Revs. Modern Phys. **26**, 95 (1954).

values of $p_{3/2}$ and $p_{1/2}$.⁶ These levels bracket the 2.01-Mev level which from shell model considerations we take to be the $f_{5/2}$ state. The $g_{9/2}$ level assignment is the hardest to make. In ${}_{39}\text{Y}^{89}$, the $p_{1/2}-g_{9/2}$ spacing is experimentally fixed at 0.913 Mev.⁷ Y^{89} has a magic neutron core and closed proton subshells up to but not including $2p_{1/2}$ and one $2p_{1/2}$ proton. The levels are therefore close to single-particle levels and the spin of the excited state is fixed by the fact that it is isomeric. It is hard to say what this spacing corresponds to in Ca^{41} since the mass number A is so different. Two effects that are certainly present are: (a) the oscillator level spacing increases for Ca^{41} thus tending to increase the $p_{1/2}-g_{9/2}$ separation; (b) the spin-orbit interaction increases⁸ thus tending to decrease the $p_{1/2}-g_{9/2}$ separation in Ca^{41} (i.e., $g_{9/2}$ is pushed down further and $p_{1/2}$ is pushed up further). As a guess the 2.89 Mev level in Ca^{41} was taken to be the $g_{9/2}$ state, thus corresponding to a $p_{1/2}-g_{9/2}$ separation of 0.42 Mev. The $g_{9/2}$ level is probably not lower than 2.89 Mev. It resulted that with the $g_{9/2}$ level taken at this value the spin 6, 4, and 2 states of Ca^{42} were not appreciably influenced by its presence. The effect of the $g_{9/2}$ level on the spin-zero state, while considerable, did not vary appreciably if the g level were raised up by one Mev. With the $g_{9/2}$ state at 2.89 Mev the spin-zero ground state in Ca^{42} contained a 9% admixture of the $g_{9/2}^2$ wave function.

In order to fix the position of the $g_{7/2}$ level in Ca^{41} , it was thought best to compute the $g_{9/2}-g_{7/2}$ doublet splitting from theoretical considerations and experiments designed to measure this splitting. Harvey⁹ finds the energy discontinuity in neutron binding energy at magic number 50 (i.e., the $g_{9/2}-g_{7/2}$ splitting) to be 2 Mev for cores of 86 and 84 particles. We wish the splitting for a core of 40 particles. Assuming the spin-orbit splitting goes as $A^{-2/3}$,⁸ we get a splitting of 3.2 Mev for the Ca^{40} core. Alternately, taking the 2-Mev f -state splitting for Ca^{41} as given and assuming a $(2l+1)$ dependence on the splitting for fixed A , we get a $g_{9/2}-g_{7/2}$ splitting of 2.6 Mev. These values are sufficiently close for the purposes of this calculation, so we arbitrarily assigned a value of 3 Mev to the $g_{9/2}-g_{7/2}$ splitting and thus took the $g_{7/2}$ state of Ca^{41} to be at 5.89 Mev. The $2d_{5/2}$ state has 2 nodes to one node for the $1f_{7/2}$ state, thus giving a small overlap. In addition it is assumed to be far away in energy, and we therefore neglect its contribution to the calculation. Although the $g_{7/2}$ state is just as far away in energy from the $f_{7/2}$ state, it has only one node and almost exactly overlaps the $f_{7/2}$ state (see Fig. 1). Hence we keep it in the calculation. Higher excited single-particle states of the Ca^{41} odd neutron were neglected because they were supposed to be too far away in energy or else overlapped

the $f_{7/2}$ state badly. Parity considerations also decrease the coupling between the f configurations and those in the next shell. Consider Ca^{42} with a zero-order f^2 configuration. In order to couple with f^2 , the configurations in the next higher shell must have plus parity. This immediately dispenses with the fg , fs , and fd configurations and leaves the configurations g^2 , gd , etc., which lie two times higher in energy than the odd-parity levels and in general have small interaction matrix elements with the f^2 configuration.

The states in Ca^{41} corresponding to core excitations have been discussed in the introduction and are neglected for the reasons referred to there.

II. LEVELS OF Ca^{42}

Schiffer¹⁰ finds levels in Ca^{42} at 1.51 ± 0.03 , 1.95 ± 0.07 , 2.29 ± 0.05 , 2.59 ± 0.07 , 3.02 ± 0.05 , and 3.75 ± 0.07 Mev.¹¹ The 1.51-Mev level has an experimental spin assignment of 2 from beta-gamma angular correlations.¹² To zero order the lowest states of Ca^{42} should correspond to an f^2 configuration with spins 0, 2, 4, and 6. (No odd spins due to the Pauli principle.) Any reasonable assumption for the interparticle forces together with any strength of surface coupling will give the level order 0, 2, 4, 6.¹³ The third and fourth excited states of Ca^{42} were accordingly assumed to have spins 4 and 6. The identification of the spin-six level is the least certain since the lowest levels of the $f_{7/2}p_{3/2}$ configuration must lie nearby. However, the position of this level is sufficiently uncritical for the purposes of predicting the levels of Ca^{43} that an error of a few tenths of a Mev will not change the computed Ca^{43} levels appreciably. The experimental relative level spacings are shown in Fig. 2. In order to fix the absolute value of the ground-state energy of Ca^{42} , information on binding energies¹⁴ was used. On the basis of the model used here, the two neutrons in Ca^{42} core are each bound to the core by the energies of the Ca^{41} nucleus. These

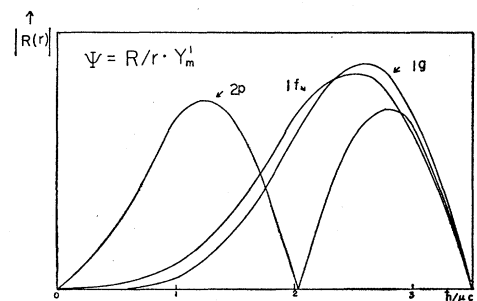


FIG. 1. Radial wave functions for the f , p , and g states of Ca^{41} where the central potential is constant and the nuclear wall is an infinite barrier.

⁶ J. R. Holt and T. N. Marsham, Proc. Phys. Soc. (London) **A66**, 565 (1953).

⁷ Evidence summarized by M. Goldhaber and R. D. Hill, Revs. Modern Phys. **24**, 179 (1952).

⁸ D. R. Inglis, Revs. Modern Phys. **25**, 390 (1953).

⁹ J. A. Harvey, Phys. Rev. **81**, 353 (1951).

¹⁰ J. P. Schiffer, Phys. Rev. **97**, 428 (1955).

¹¹ Braams and Buechner find levels at 1.53, 1.84, and 2.43 Mev. This information reached the authors after the calculations had been performed. They would not change the results appreciably.

¹² D. T. Stevenson and M. Deutsch, Phys. Rev. **84**, 1071 (1951).

¹³ Dieter Kurath, Phys. Rev. **91**, 1430 (1953).

¹⁴ Summarized in reference 13.

bonds we call core bonds. In addition there is an extra binding due to the interparticle force. This binding is due to the particle bond. The ground state binding energy due to the core and particle bonds in Ca^{42} is simply the difference between the binding energies of Ca^{42} and Ca^{40} which is 19.8 Mev. Hence we take $E_0 = -19.8$ Mev for Ca^{42} . Then the Hamiltonian $H_0 + V$ for the Ca^{42} problem has a lowest state at -19.8 Mev. It is more convenient to write $H_0 = -16.6$ Mev $+ \Delta H_0$ since the $f_{7/2}$ neutron in Ca^{41} has an 8.3-Mev binding energy. This makes $\Delta H_0 = 0$ for the $f_{7/2}^2$ configuration and positive for all other configurations. Our problem is then to find the eigenvalues of $\Delta H_0 + V$ with lowest state at -3.2 Mev. The -3.2 Mev can be looked at as the contribution to the energy due to the particle bond alone.

III. SOLUTION OF THE TWO-BODY PROBLEM

As a first approximation we shall consider the effects of the $f_{5/2}$, $g_{9/2}$, and $g_{7/2}$ states on the zero-order $f_{7/2}^2$ configuration in Ca^{42} . As shown in Fig. 1, the radial dependence of the g state is almost identical to that of the f state. We shall assume they are identical and thus all radial integrals will be independent of l , the orbital quantum number.

We now make substitutions into Eq. (11) of I. The values of l_1, l_2 of interest are only f^2 , and g^2 , since the state fg has odd parity. It is easier to work with the expression

$$\beta(Jl_1l_2) = \frac{1}{\alpha(Jl_1l_2)} = \left\{ \sum_{j_1'j_2'} \frac{|(l_1l_2J|j_1'j_2'l_1l_2)|^2}{E_J - H_0(l_1l_2j_1'j_2')} \right\}^{-1}. \quad (1)$$

Then, by a slight manipulation of Eq. (11) in I, we get

$$\begin{vmatrix} (f^2J|V|f^2J) - \beta(Jf^2) & (f^2J|V|g^2J) \\ (g^2J|V|f^2J) & (g^2J|V|g^2J) - \beta(Jg^2) \end{vmatrix} = 0. \quad (2)$$

From the data given in Secs. I and II plus the values of $LS-jj$ transformation coefficients,¹⁵ one can easily evaluate the β 's. Equation (2) represents four equations, one for each value of J . In order to get unique answers, we express our unknown matrix elements in terms of the four matrix elements V_J , where

$$(f^2J|V|f^2J) \equiv V_J \quad (3)$$

and $|f^2J\rangle$ is a two-particle wave function in an LS

TABLE I. Values of $A_{\kappa J}$ to three decimal places. $F^\kappa = \sum_J A_{\kappa J} V_J$.

$\kappa \setminus J$	0	2	4	6
0	-0.103	0.204	0.367	0.529
2	0.766	-1.457	-3.448	4.147
4	2.017	-5.034	1.845	1.181
6	2.276	4.716	0.940	-7.948

¹⁵ G. Racah, *Physica* **16**, 651 (1950).

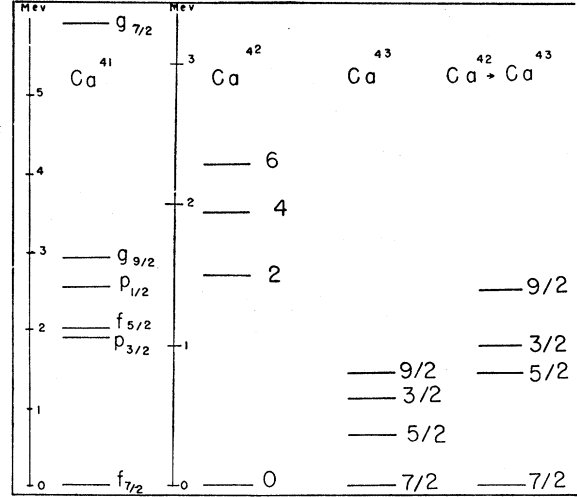


FIG. 2. The first three level diagrams on the left give the level spacings and spin assignments of Ca^{41} , Ca^{42} , and Ca^{43} which are taken as the "empirical" levels. The diagram on the right represents the predicted level spacings of Ca^{43} based on the empirical levels of Ca^{42} if configuration interaction is neglected.

representation for $l_1 = l_2 = 3, S = 0, L = J$. Now each V_J can be expressed in terms of four Slater parameters¹⁶ and inversely the Slater parameters F^κ , ($\kappa = 0, 2, 4, 6$) can be expressed in terms of V_J . The F^κ 's are the radial integrals of the problem and are independent of l_1, l_2 as pointed out above. These relations can be written:

$$V_J = \sum_\kappa B_{J\kappa} F^\kappa, \quad F^\kappa = \sum_J A_{\kappa J} V_J. \quad (4)$$

$B_{J\kappa}$ is given in Condon and Shortley¹⁶ and $A_{\kappa J}$ is given in Table I. We also need expressions for F^κ for $\kappa = 1, 3, 5, 7, 8$. In general, F^κ is a smooth function of κ . In fact, for zero-range forces, $F^\kappa = (2\kappa + 1)F^0$. Examples of Slater parameters appear in Kurath's¹³ work. We therefore take the values of F^κ for $\kappa = 1, 3, 5, 7, 8$ to be given by linear interpolation or extrapolation on the F^κ 's for $\kappa = 0, 2, 4, 6$, i.e.,

$$\begin{aligned} F^1 &= \frac{1}{2}(F^0 + F^2), & F^5 &= \frac{1}{2}(F^4 + F^6), & F^8 &= 2F^6 - F^4, \\ F^3 &= \frac{1}{2}(F^2 + F^4), & F^7 &= \frac{1}{2}(3F^6 - F^4). \end{aligned} \quad (5)$$

Now all the relevant Slater parameters can be expressed in terms of the four V_J 's. The matrix elements $(g^2J|V|g^2J)$ can be expressed in terms of $F^\kappa, \kappa = 0, 2, 4, 6, 8$. The matrix elements $(g^2J|V|f^2J)$ can be expressed in terms of $F^\kappa, \kappa = 1, 3, 5, 7$. Hence we finally write all matrix elements in terms of $V_J, J = 0, 2, 4, 6$ and then solve for V_J . The expressions for $(g^2J|V|g^2J)$ in terms¹⁷ of F^κ and the other diagonal matrix elements¹⁶ are given in the literature and the off-diagonal elements are given in Table II. Equation (2) can now be solved in a straightforward manner and one finds for the values

¹⁶ E. U. Condon and G. H. Shortley, *The Theory of Atomic Spectra* (Cambridge University Press, Cambridge, 1951).

¹⁷ G. H. Shortley and B. Fried, *Phys. Rev.* **54**, 739 (1938).

TABLE II. Off-diagonal matrix elements of a singlet central force in LS coupling. $R^{(a)}(l_1l_2; l_3l_4)$ is defined as on p. 175 of Condon and Shortley.¹⁶

$$\begin{aligned}
 (f^2|V_J|fp) &= -(2/5)(42)^{1/2}W(3331; J2)R^{(2)}(f^2; fp) \\
 &\quad - 4(7/33)^{1/2}W(3331; J4)R^{(4)}(f^2; fp) \\
 (f^2|V_J|p^2) &= (9/5)W(3311; J2)R^{(2)}(f^2; p^2) \\
 &\quad + (4/3)W(3311; J4)R^{(4)}(f^2; p^2) \\
 (f^2|V_J|g^2) &= -4W(4433; J1)R^{(1)}(f^2; g^2) \\
 &\quad - (18/11)W(4433; J3)R^{(3)}(f^2; g^2) \\
 &\quad - (180/143)W(4433; J5)R^{(5)}(f^2; g^2) \\
 &\quad - (245/143)W(4433; J7)R^{(7)}(f^2; g^2) \\
 (p^2|V_J|fp) &= -\frac{1}{2}\sqrt{3}W(1131; J2)R^{(2)}(p^2; fp) \\
 (g^2|V_J|fp) &= 12(3/77)^{1/2}W(4431; J3)R^{(3)}(g^2; fp) \\
 &\quad + 30/11(6/13)^{1/2}W(4431; J5)R^{(5)}(g^2; fp) \\
 (g^2|V_J|p^2) &= -(12/7)W(4411; J3)R^{(3)}(g^2; p^2) \\
 &\quad - (15/11)W(4411; J5)R^{(5)}(g^2; p^2)
 \end{aligned}$$

of V_J and $\beta(J, f^2)$.

$$\begin{aligned}
 V_0 &= -3.33 \text{ Mev}, & \beta(0, f^2) &= -4.20 \text{ Mev}, \\
 V_2 &= -2.49 \text{ Mev}, & \beta(2, f^2) &= -2.50 \text{ Mev}, \\
 V_4 &= -2.10 \text{ Mev}, & \beta(4, f^2) &= -2.16 \text{ Mev}, \\
 V_6 &= -2.20 \text{ Mev}, & \beta(6, f^2) &= -2.22 \text{ Mev}.
 \end{aligned} \tag{6}$$

We note that only V_0 differs much from the corresponding $\beta(0, f^2)$. The $\beta(J, f^2)$'s are the V_J 's one would find if only the $f_{5/2}$ state were taken into consideration. In other words, it is the spin-zero ground state of Ca^{42} that is most affected by the presence of the states $g_{9/2}$ and $g_{7/2}$. The other states are hardly influenced at all.

In order to find the effect of the p states we need to know the radial integrals involved in the matrix elements like $(f^2J|V|fpJ)$ and $(f^2J|V|p^2J)$. An upper limit on these matrix elements can be established by assuming that the p state radial wave function is identical to the f state radial wave function. In this case, the matrix elements can be expressed in terms of the V_J 's by the methods described above. In this limit, the p states still leave V_4 and V_6 unchanged and change V_2 from -2.49 Mev to -2.47 Mev. Since the overlap is only the order of 50 percent [see Fig. 1], we will take $V_2 = -2.48$ Mev. The general accuracy of our calculation is such that more detailed investigation of this point is not necessary. In a similar fashion, it was estimated that V_0 is changed from -3.33 Mev to -3.25 Mev. The fact that V_0 sustained the greatest change again reflects the fact that the spin-zero ground state of Ca^{42} is the most strongly affected state by configuration interaction. Finally we list here our semiempirically determined values of V_J .

$$\begin{aligned}
 V_0 &= -3.25 \text{ Mev}, & V_2 &= -2.48 \text{ Mev}, \\
 V_4 &= -2.10 \text{ Mev}, & V_6 &= -2.20 \text{ Mev}.
 \end{aligned} \tag{7}$$

It is interesting to compute the diagonal matrix elements for the Ca^{42} configurations $f_{7/2}^2$ ($J=0, 2, 4, 6$) since the difference between these values and energies for these states is the energy due to configuration interaction. This comparison is shown in Fig. (3).

We can also fit a potential well to our empirically derived diagonal matrix elements. Let D_J be the diagonal element for spin J in a jj representation. We then have:

$$\begin{aligned}
 D_0 &= -1.86 \text{ Mev}, & D_2 &= -1.27 \text{ Mev}, \\
 D_4 &= -0.77 \text{ Mev}, & D_6 &= -0.31 \text{ Mev}.
 \end{aligned} \tag{8}$$

We have given graphs of D_J for various assumed potentials in I. It is important to notice that $(D_2 - D_0)/(D_4 - D_2) = 1.18$ while $(E_2 - E_0)/(E_4 - E_2) = 3.43$. We see that we must fit to two almost equal spacings and not to a ratio of 3.43 which would be the case if configuration interaction were neglected. In Table III are listed the best fits for potentials of the form $V_0 \exp[-r^2/r_0^2]$. These tables were computed from Kurath's¹³ evaluation of the Slater parameters for the above potential using oscillator wave functions which go as $r^3 \exp[-r^2/r_n^2]$. The parameter $\lambda = r_0/r_n$ measures the ratio of the force range to the spread of the nuclear wave function. The best value of λ lies between 1.11 and 1.25. A good fit is obtained with $V_0 = -14.4$ Mev, $\lambda = 1.18$. If in addition we demand that this well have a bound state at zero energy thus approximating the singlet well binding strength we obtain an effective range $r_{\text{eff}} = 4 \times 10^{-13}$ cm and $r_0 = 2.79 \times 10^{-13}$ cm.

On the other hand it seems more realistic to fix r_n at some value consistent with the radius of Ca. Kurath¹³ has proposed a value of $r_n = 2.9 \times 10^{-13}$ cm on the basis of best approximating a square well wave function whose constants are determined from the experimental evidence in the mass number 40 region. This value of r_n gives for the mean square radius, $\langle r^2 \rangle^{1/2}$, 4.35×10^{-13} cm, which is to be compared with an "outside" radius of 4.95×10^{-13} cm for $A = 43$, based on $R = \bar{r} \times A^{1/3}$, with $\bar{r} = 1.41 \times 10^{-13}$ cm. Since $\lambda = 1.18$, we find the range of the interparticle Gaussian potential is $r_0 = 3.42 \times 10^{-13}$

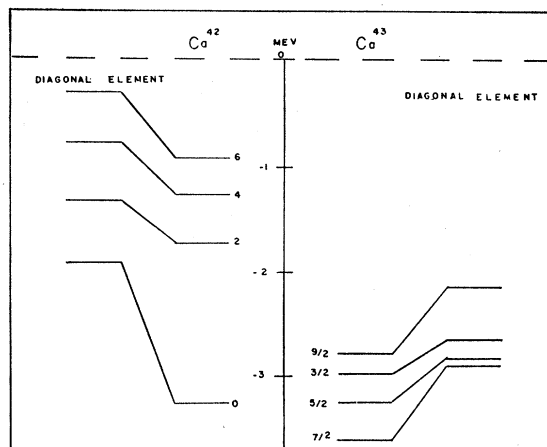


FIG. 3. The level diagrams on the outside represent the contribution due to diagonal matrix elements alone to the observed levels. The difference between these energies and the total energies is due to configuration interaction. The levels labeled by spin values are the observed levels.

cm. Combining this with the well depth of 14.4 Mev, we find a well depth parameter¹⁸ $s=1.5$ (i.e., this potential is strong enough to bind two particles) and effective range of 3.82×10^{-13} cm. Fitting a Gaussian to low-energy singlet scattering data one finds $V_0=35$ Mev, $r_{\text{eff}}=2.7 \times 10^{-13}$ cm, and $r_0=1.78 \times 10^{-13}$ cm. If our results are correct we must conclude that the effective nuclear interaction potential in Ca⁴² is indeed not well represented by a Gaussian constructed to fit the low-energy scattering data but is better represented by a Gaussian which is about one-half as deep and two times longer-ranged. There are two possible explanations for this result:

(1) The presence of the core excitations which were neglected in the calculation cause the modifications. This effect is predicted theoretically³ but it remains to be calculated for the case of Ca⁴². In particular, collective core excitations should be in the direction to produce an effectively longer-range interaction. (Compare figures showing energy shifts in papers I and II.)

(2) The relative energies involved between the extra core particles are so great that a potential which fits low-energy scattering only is inappropriate.

It is a simple matter to investigate this second point further since, as shown by Talmi,¹⁹ the independent-particle two-body wave functions corresponding to a harmonic oscillator central potential can be easily expressed in terms of the relative (\mathbf{r}) and center-of-mass (\mathbf{R}) coordinates of the two particles. The two-particle wave function can always be written in the form

$$\psi(\mathbf{r}_1, \mathbf{r}_2) = \sum_n \alpha_n \phi_n(\mathbf{R}) \chi_n(r), \quad (9)$$

where ϕ and χ are themselves harmonic oscillator wave functions. If χ corresponds to a $1s$ state of relative motion, then one finds a probability distribution of relative energies given by:

$$p(\epsilon) d\epsilon = 4(2/\pi)^{3/2} (\hbar\omega)^{-3} \exp[-2\epsilon/\hbar\omega] \epsilon^{1/2} d\epsilon, \quad (10)$$

where ϵ is the center-of-mass kinetic energy of the two

TABLE III. Diagonal matrix elements predicted for an $(f_{7/2})^2$ configuration with $J=0, 2, 4, 6$ using a Gaussian potential of the form $V_0 \exp[-r^2/r_0^2]$ and an oscillator wave function of the form $\psi \sim r^3 \exp[-r^2/r_n^2]$. The best value of V_0 is listed for the given values of λ ($\lambda=r_0/r_n$) such that the predictions agree most closely with the matrix elements deduced from the empirical analysis. All numbers but the dimensionless values of λ are in -Mev.

Empirical analysis	V_0	18.6	15.8	14.4	13.3	11.9
λ		1.00	1.11	1.18	1.25	1.33
0.31	D_6	0.35	0.37	0.38	0.38	0.39
0.77	D_4	0.59	0.66	0.70	0.74	0.78
1.27	D_2	1.14	1.22	1.27	1.30	1.33
1.86	D_0	1.92	1.88	1.87	1.84	1.82

¹⁸ J. M. Blatt and V. F. Weisskopf, *Theoretical Nuclear Physics* (John Wiley and Sons, Inc., New York, 1952), p. 55.

¹⁹ I. Talmi, *Helv. Phys. Acta* **25**, 185 (1952).

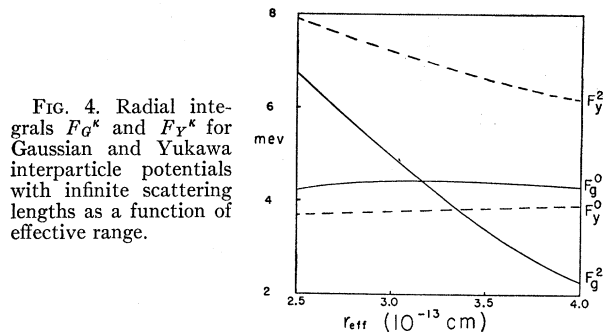


FIG. 4. Radial integrals F_G^k and F_Y^k for Gaussian and Yukawa interparticle potentials with infinite scattering lengths as a function of effective range.

particles and $\hbar\omega$ is the characteristic energy spacing of the single-particle central oscillator well. The average energy is $\bar{\epsilon} = \frac{3}{4} \hbar\omega$. Equating the energy of the top particle in the well to a Fermi energy of 30 Mev, we find $\hbar\omega=8.6$ Mev for O¹⁷ and $\hbar\omega=6.7$ Mev for Ca⁴¹. (Elliott and Flowers²⁰ use 7 Mev and Redlich²¹ uses 10 Mev for O¹⁷.) The average relative scattering energy then amounts to 6.45 Mev in O¹⁷ and 5 Mev in Ca⁴¹. These numbers are *lower limits* on the average scattering energy since they are based on a $1s$ state of relative motion. Since the shape-independent analysis of pp scattering breaks down around 10 Mev, some shape dependence for the effective nuclear interaction is to be expected.

The shape dependence of the matrix elements can also be demonstrated by computing them with a Gaussian and a Yukawa potential, both adjusted to give the same effective range and scattering length. This calculation was performed for the $1p^2$ radial integrals. The scattering length of both potentials was chosen to be infinite, thus corresponding to a bound state at zero energy, and the results are plotted as a function of the effective range in Fig. 4. The integrals plotted are given by Swiatecki.²² The parameter r_n giving the range of the nuclear wave function was taken to be 2.33×10^{-13} cm. ($r_n = \sqrt{2} a_0$ in Lane's notation²³) following the results of Elliott in fitting Coulomb energy data in the $1p$ shell as reported by Lane.²³ Table IV gives the diagonal matrix elements for the states $1p_{3/2}^2 J=0, 2$ which are derived from the corresponding radial integrals. It is immediately seen that F^0 is not very shape dependent while F^2 has a considerable shape dependence for the larger effective ranges. For a very slowly varying potential all F^k 's are very much smaller than F^0 , and for a delta function potential $F^k = (2k+1)F^0$. Thus, roughly speaking, the values of F^k for $k>0$ should be expected to increase as the potential is made to vary more rapidly with r . The trends in Fig. 4 can be interpreted as reflecting this. Longer effective ranges correspond to less rapidly varying

²⁰ B. H. Flowers, lecture at University of Chicago, March, 1955 (unpublished).

²¹ M. Redlich, *Phys. Rev.* **95**, 448 (1954).

²² W. J. Swiatecki, *Proc. Roy. Soc. (London)* **A205**, 238 (1951).

²³ A. M. Lane, *Proc. Phys. Soc. (London)* **A68**, 197 (1955).

TABLE IV. Diagonal matrix elements in Mev for the spin zero and two states of the $1p_{3/2}^2$ configuration using Gaussian and Yukawa potentials with infinite scattering lengths and effective ranges in 10^{-13} cm as shown in the first column. The wave functions used are described in the text. Δ_G and Δ_Y are the first-order energy spacings for the Gaussian and Yukawa wells and the last column gives the percent difference in these spacings.

r_{eff}	$D_0(G)$	$D_0(Y)$	$D_2(G)$	$D_2(Y)$	Δ_G	Δ_Y	% difference
2.5	4.62	4.60	1.48	1.34	3.14	3.26	3.7
3.0	4.26	4.45	1.53	1.35	2.73	3.10	13
3.5	3.81	4.32	1.50	1.36	2.31	2.96	25
4.0	3.48	4.25	1.46	1.39	2.02	2.86	34

potentials and a Yukawa well varies more rapidly than a Gaussian. Configurations involving higher angular momenta also require radial integrals F^κ for higher values of κ in order to express their matrix elements. Hence energy levels corresponding to higher configurations should show an increasing shape dependence. From Fig. 4 and Table IV one sees that if the effective two-body singlet potential acting between $1p$ nucleons has an effective range near 2.7×10^{-13} cm (the singlet scattering effective range) then one can expect a slight shape dependence for the matrix elements. However, if for some reason the effective range of the internucleon potential in nuclear matter is closer to 4×10^{-13} cm, then the problem becomes considerably shape-dependent.

Comparing the empirical values of D_J with the predictions of the modified Gaussian wells in I, we see that the "singulated Gaussian" cannot possibly fit the data and the "hard core Gaussian" gives a best fit around $\lambda=0.79$. Especially for high l , the shape dependence of the results is sufficient to raise the hope that studies of nuclear energy levels may yield information on the shape of the potential. This point is under further study.

The wave functions for the four states of Ca^{42} can be written out in the L - S or jj coupling representations. The mixture parameters [defined in Eq. (16) of I for the case of jj coupling] resulting from the semi-empirical values of V_J given above are given in Tables V and VI.

IV. Ca^{43} AND THE THREE-BODY PROBLEM

The level energies and spin assignments given by Lindqvist and Mitchell²⁴ supplied the necessary infor-

TABLE V. Mixture parameters for the spin 0, 2, 4, and 6 states of Ca^{42} in the L - S coupling representation based on the semi-empirical analysis of the levels of Ca^{41} and Ca^{42} .

J	$f^2 1J$	$f^2 3(J-1)$	$f^2 3(J+1)$	$g^2 1J$	$g^2 3(J+1)$
0	0.884	...	-0.315	-0.335	0.098
2	0.896	0.351	-0.276	0	0
4	0.872	0.455	-0.194	0	0
6	0.864	0.503	...	0	0

²⁴ T. Lindqvist and A. C. G. Mitchell, Phys. Rev. **95**, 1535 (1954).

mation about Ca^{43} . They find levels at 0.369, 0.627, and 0.81 Mev with spins 5/2, 3/2, and 9/2 in that order. The ground state spin of 7/2 and magnetic moment of -1.3152 ± 0.0002 nm come from the work of Jeffries.²⁵ Levels at 0.38 and 0.61 are seen by Braams.²⁶

A very general test of the presence of configuration interaction independent of the exchange properties or space dependence of the two body potential was described in Sec. IV of I. If configuration interaction is small the relations between the levels of Ca^{42} and Ca^{43} should be simply given in terms of fractional parentage coefficients. One might name the levels of Ca^{43} predicted from those of Ca^{42} , assuming pure configurations, "projected" levels. As shown in Fig. 2, the projected levels of Ca^{43} are not in good agreement with the observed levels (although the level order is the same). This proves that there exists no two-body potential which can predict the observed level spacings of both Ca^{42} and Ca^{43} and give negligible configuration interaction within the framework of the independent particle model.

The two-body analysis of Sec. III of I can be generalized to include three bodies so that Ca^{43} could be

TABLE VI. Mixture parameters of the states of Ca^{42} in a jj representation based on the semiempirical analysis of the levels of Ca^{41} and Ca^{42} .

J	$f_{1/2}^2$	$f_{1/2}f_{5/2}$	$f_{5/2}^2$	$g_{9/2}^2$	$g_{7/2}^2$
0	0.87	...	0.34	-0.31	-0.15
2	0.948	-0.212	0.238	0	0
4	0.915	-0.369	0.170	0	0
6	0.794	-0.610	...	0	0

treated in a manner similar to Ca^{42} . There result four equations for the same unknowns V_0 , V_2 , V_4 , and V_6 . In this case the coefficients in these equations involve the empirically given energies of the excited states of Ca^{41} and Ca^{43} instead of the states of Ca^{41} and Ca^{42} . One can solve for the V_J 's and compare with those found from the Ca^{42} analysis. Alternatively one can eliminate the V_J 's from the equations and obtain relations between the levels of Ca^{42} and Ca^{43} . These relations would then include the effects of configuration interaction. This approach will not be reported on further in this paper but instead a less elegant but more straightforward one is used.

Since all the two-body matrix elements are given as linear functions of V_J , we can apply Eq. (15) of I and obtain all the three-body matrix elements as linear functions of V_J . It then remains to diagonalize the resulting Ca^{43} matrices of the Hamiltonian. Upon calculating the various matrix elements, it was found that most of the nondiagonal elements were quite small with some notable exceptions. A series of transformations was

²⁵ C. D. Jeffries, Phys. Rev. **90**, 1130 (1953).

²⁶ C. M. Braams, Phys. Rev. **95**, 650 (1954).

then applied to the matrix in question to reduce the magnitude of the larger nondiagonal elements below a certain preassigned value. When this process was completed the eigenvalues were obtained by using second order perturbation formulas. The results of this calculation and comparison with the experiments are shown in Table VII and Fig. 3. The spacings and spin assignments agree remarkably well with the experimental results. The difference in binding energy between Ca^{43} and Ca^{40} is 27.8 Mev. Subtracting out the 3.57 Mev calculated for the particle forces and dividing by three leaves 8.08 Mev for the single-particle bond rather than the 8.3 Mev used for Ca^{42} . This can be interpreted to mean that the single-particle bond has a dependence on the number of nucleons A . If we assume the $1/A$ dependence discovered by Kurath¹³ in his analysis of the binding energies in the $f_{7/2}$ shell, then the 8.3-Mev bond in Ca^{42} would be an 8.1-Mev bond in Ca^{43} which agrees quite well with the calculated results.

The almost exact agreement between experiment and theory is probably fortuitous. First, the perturbation method of obtaining eigenvalues is only accurate to about 0.02 Mev. Secondly, some errors in the "em-

TABLE VII. Comparison of calculated and experimental energies for Ca^{43} in Mev. The experimental energy for the $J=7/2$ state is normalized to the calculated result. The diagonal matrix elements are given in order to illustrate the effect of configuration interaction.

J	Experimental ^a energies	Calculated energies	Diagonal matrix elements
7/2	-3.57	-3.57	-2.84
5/2	-3.20	-3.19	-2.77
3/2	-2.94	-2.96	-2.63
9/2	-2.76	-2.77	-2.13

^a See reference 24.

pirical" levels of Ca^{41} and Ca^{42} are probably present. (Position of $g_{9/2}$ state in Ca^{41} , spin 6 state in Ca^{42} , etc.) Thirdly, the odd-state tensor force discussed in I has been neglected. This error is considerably reduced by the small triplet admixtures in the final wave functions as shown in Table V. Consider the spin-zero state of Ca^{42} . In zero order (pure $f_{7/2}^2$) it contains a 43 percent triplet admixture but this decreases to a 10 percent admixture in the final wave function. Since the tensor force is a triplet interaction and gives no contribution in singlet states, its effect is greatly diminished compared to its effect on a zero-order state which is given in Fig. 4 of I.

In order to investigate further the influence of triplet forces, the following idealized problem was solved: The Hamiltonian was taken to be

$$H = H_0 + aP_S + bP_T, \quad (11)$$

where P_S and P_T are singlet and triplet projection operators, a and b are numbers measuring the singlet and triplet potential strengths, and H_0 has two single-

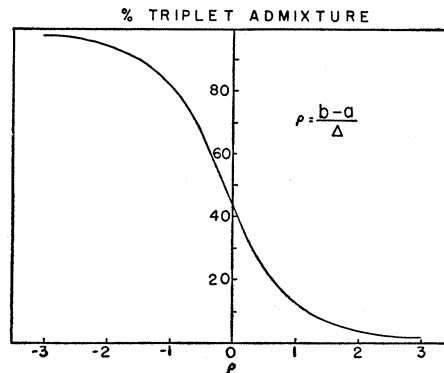


FIG. 5. Percent of triplet component (P) in the lowest spin zero wave function corresponding to the Hamiltonian of Eq. (11). ρ is defined just under Eq. (11).

particle levels $f_{7/2}$ and $f_{5/2}$ separated by an energy $\Delta/2$. The two-body two-by-two energy matrix for the spin-zero state was set up and the percent of triplet state admixture P was computed. P is a function of one parameter ρ , where $\rho = (b-a)/\Delta$. $P(\rho)$ is shown in Fig. 5. In the case of Ca^{42} we take $a = \beta(f^2_0) \sim -4$ Mev where $\beta(f^2_0)$ is given in Eq. (6). Δ is 4 Mev and $b=0$ which gives a 12% triplet admixture. Now if a repulsive triplet force is added, the amount of triplet admixture decreases. For instance, if $b=2$ Mev we get a 7% triplet admixture. As mentioned in I, scattering data implies that the triplet odd-state force (triplet even forces do not occur between neutrons due to the Pauli principle) is indeed repulsive. We conclude that the neglect of triplet forces in the calculation is a good approximation, owing to the fact that the predominantly singlet forces tend to create predominantly singlet wave functions.

The ground state of Ca^{43} was further investigated in order to find its magnetic moment. The general formulas for calculating three-body magnetic moments are given in Sec. V of I. The admixtures $f_{7/2}^2(2)f_{5/2}$, $f_{7/2}^2(4)f_{5/2}$ and $f_{7/2}^2(6)f_{5/2}$ (the number in parentheses gives the value of J to which $f_{7/2}^2$ is coupled before being coupled to $f_{5/2}$ to make a total J of $7/2$) are the only ones which are coupled to the $f_{7/2}^3$ dominant mode by the magnetic moment operator defined in Eq. (19) of I. These admixtures are mainly responsible for the shift of the magnetic moment from the Schmidt line value given by $\langle f_{7/2}^3 7/2 | \mu | f_{7/2}^3 7/2 \rangle = -1.91$ nm because they contribute a value linear in the mixture amplitudes while other states can only give a contribution quadratic in the mixture amplitudes. The state $f_{5/2}^2(0)f_{7/2}$ was the only state not directly coupled to the $f_{7/2}^3$ state that gave an appreciable contribution to the magnetic moment. The magnitudes of the relevant mixture parameters and the contribution of each admixture to the magnetic moment (both diagonal and off-diagonal) are given in Table VIII.

We also include a small correction due to the motion of the core about the common center of mass of core and extra core particles, because it is easy to include

TABLE VIII. Magnetic moment contributions of the various admixed states to the ground state of Ca^{43} in nuclear magnetons. The empirical value is -1.315 (reference 25).

Admixed state	Mixture amplitude	Magnetic moment contribution
$7/2^2(2)5/2$	-0.025	+0.033
$7/2^2(4)5/2$	-0.081	+0.211
$7/2^2(6)5/2$	-0.108	+0.271
$5/2^2(0)7/2$	-0.209	-0.117
$7/2^2$	0.961	-1.764
Center-of-mass motion		+0.061
	Total	-1.305

approximately, although other omitted effects may contribute corrections of the same order of magnitude. The magnetic moment of a system composed of an extra core particle structure and a core is given by

$$\mu = g_c \langle I_c \rangle + g_J \langle I_J \rangle, \quad (12)$$

where g_c and g_J are the gyromagnetic ratios for the core and particle structure respectively and I_c and I_J are their total angular momenta about the center of mass of the system. This magnetic moment can be split up into two parts μ_1 and $\Delta\mu_c$, where

$$\mu_1 = g_J \langle I_c + I_J \rangle = g_J I_{\text{total}}, \quad \Delta\mu_c = (g_c - g_J) \langle I_c \rangle. \quad (13)$$

Now μ_1 is the part computed when one assumes the total angular momentum is associated with the particle structure and $\Delta\mu_c$ is the correction term associated with a nonvanishing value of I_c . g_c is taken to be Z/A and g_J is taken to be -0.377 . $\langle I_c \rangle$ we approximate as $3\hbar/A$, since the dominant state (${}^2F_{7/2}$, seniority 1) represents an orbital angular momentum of three units carried in effect by one particle. In this way, we obtain the crude estimate for $\Delta\mu_c$:

$$\Delta\mu_c = 0.061 \text{ nm}. \quad (14)$$

The agreement of the predicted and observed magnetic moments is nearly perfect and surely better than one could have expected. It shows, however, that the configuration mixing obtained for the ground state must be of the right order of magnitude.

Two low-lying levels in Ca^{43} , so far unobserved, may be predicted by using the same empirically determined matrix elements. These have spins $11/2$ and $15/2$, and predicted energies above the ground state,

$$E_{11/2} = 0.835 \text{ Mev}, \quad E_{15/2} = 1.00 \text{ Mev}.$$

V. SURFACE COUPLING

The results of II were employed to try to obtain a fit to the data with a combination of direct coupling and surface coupling. Best fits to energies and magnetic moment were obtained with zero surface coupling. A rough upper limit to the strength of coupling is expressed by

$$\hbar\omega \gtrsim 15 \text{ Mev}, \quad (15)$$

where $\hbar\omega$ is the surfon energy, and the mass parameter

B and coupling parameter k are defined as in II. With stronger surface coupling, one can still approximately (but not well) fit the energies, but in order to do so it is necessary to reduce the strength of direct particle coupling. This in turn reduces the directly induced configuration mixing and causes the predicted magnetic moment shift to be appreciably less than the observed shift, in spite of the surface contributions to this shift. This argument applies in the region of weak surface coupling. Still stronger coupling has not been investigated closely, but intermediate coupling would predict such a large 0-2 spacing in Ca^{42} that the additional particle forces required would be unreasonably small. In the region of strong surface coupling, the surface induced 0-2 spacing would decrease again, but difficulties would arise in accounting for the relative spacings in Ca^{42} and for the level order in Ca^{43} . There is in any case no theoretical reason to expect strong surface coupling in these nuclei.

We conclude that the Ca^{40} core is an unusually rigid, undeformable, structure, like the analogous O^{16} core, for which the properties of O^{17} lead to the same conclusion.²⁵ The "hydrodynamic" value²⁶ of the surfon energy in Ca^{40} is about 4 Mev, to be compared with the limit in Eq. (15). As discussed in the introduction, however, it is not ruled out that some weak surface coupling is already included in our effective two-body potential, because of the semiempirical nature of the analysis. The only experimental test of the role of surface coupling in the calcium isotopes will be afforded by measurements of electric quadrupole effects, e.g., the $E2/M1$ ratios in γ decays in Ca^{43} or the ground-state quadrupole moment of Ca^{43} . Such data is not yet available. The problem of cascade *versus* crossover in the $3/2^- \rightarrow 7/2^-$ transitions in Ca^{43} is discussed in II.

VI. CONCLUSION

A remarkably accurate prediction of level spacings and magnetic moment of Ca^{43} has been made on the basis of the shell model perturbed by central two-body forces. Zero-order level spacings and interparticle interaction matrix elements were obtained empirically from Ca^{41} and Ca^{42} . The force was assumed to be central, two-body, and singlet for equivalent particles. The empirically determined potential appeared to be shallower and of longer range than that required to fit low-energy scattering. A study of the dependence of results on the radial shape of the potential suggests in a preliminary way that potentials with central repulsion may give a better simultaneous fit of scattering and of interparticle matrix elements in the nucleus than the Gaussian or Yukawa shapes. The analysis leads to the conclusion that surface coupling is not playing an important role in the calcium isotopes investigated. Configuration interaction is quite significant.

We have emphasized only energies and magnetic moments. Other important properties of the nuclear

states considered which will be significantly affected by configuration mixing are gamma decay rates and (p,d) or (d,p) cross sections, in addition, of course, to beta decay. These properties will need to be calculated, and similar analyses made of other nuclei in the vicinity before it can be concluded that the successful calcu-

lations reported here indeed represent an adequate description of the nuclear state.

It is a pleasure to acknowledge the many enlightening conversations we had with Professor Keith Brueckner, Dr. Richard Eden, Dr. Norman Francis, and Dr. Leonard Kisslinger.

Gamma-Ray and Neutron Yields from the Proton Bombardment of Boron

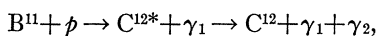
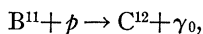
J. K. BAIR, J. D. KINGTON, AND H. B. WILLARD
Oak Ridge National Laboratory, Oak Ridge, Tennessee

(Received June 21, 1955)

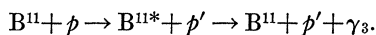
Yield curves of the gamma rays and neutrons resulting from the proton bombardment of boron have been measured for proton energies from approximately 2 to 5 Mev. Both the 0° and 90° yields for the $B^{11}(p,\gamma)C^{12}$ reaction have been measured for the ground state transition and for the transition to the 4.43-Mev state in C^{12} , as has the yield of the 2.14-Mev γ ray resulting from the inelastic scattering of protons on B^{11} . The neutron yield from $B^{11}(p,n)C^{11}$ is given at 0° and for almost 2π solid angle in the forward direction. New levels were observed in the C^{12} compound nucleus at 18.3, 18.39, 18.84, 19.2, 19.41, 19.66, 19.87, 20.25, 20.48, and 20.64 Mev. Preliminary data are given for the $B^{10}(p,n)C^{10}$ and $B^{10}(p,\gamma)C^{11}$ reactions.

I. INTRODUCTION

GAMMA-ray yield curves for B^{11} bombarded by protons have been reported by Huus and Day,¹ by Cochran, Ryan, Given, Kern, and Hahn,² and by Gove and Paul,³ who give references to earlier data. In the present work, the γ -ray yields have been extended from the previous limit of 2.8 Mev to about 5-Mev proton bombardment energy for the reactions

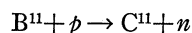


and



Measurements were made at both 0° and 90° with respect to the bombarding proton beam.

Richards, Smith, and Browne⁴ have found the threshold for the reaction



to be 3.015 ± 0.003 Mev. Blaser, Boehm, Marmier, and Scherrer⁵ have reported observation of the yield of C^{11} by a stacked foil technique. Neutron yield curves are given in the present paper for proton energies from threshold to approximately 5 Mev.

II. EXPERIMENTAL PROCEDURE

Protons from the ORNL 5.5 Mv Van de Graaff were magnetically analyzed by a 90° magnet whose

¹ Torben Huus and Robert B. Day, Phys. Rev. **91**, 599 (1953).

² Cochran, Ryan, Given, Kern, and Hahn, Phys. Rev. **87**, 672 (1952).

³ H. E. Gove and E. B. Paul, Phys. Rev. **97**, 104 (1955).

⁴ Richards, Smith, and Browne, Phys. Rev. **80**, 524 (1950).

⁵ Blaser, Boehm, Marmier, and Scherrer, Helv. Phys. Acta **24**, 465 (1951).

slits were adjusted to about 0.1 percent energy resolution. A proton moment device was used to measure the magnetic field. Energy calibration is believed to be accurate within $\pm 0.2\%$ relative to the $Li^7(p,n)Be^7$ threshold at 1.882 Mev.⁶ An electrostatic strong focus lens system was used to focus the beam on targets located 15 to 25 feet from the magnet.

Thin boron targets were prepared by evaporating elemental boron of natural isotopic ratio on tantalum backings. Target thicknesses used for the data given here were about 30 kev at 3 Mev, although thinner targets were at times used. Target thicknesses were determined by measurements on the geometrical peak of the neutron yield from a very thin target, and then comparing the yield of this and the unknown target at a proton energy where the neutron yield was slowly varying. Similar targets of 96% B^{10} were available* and were used to check that the reactions measured were due to B^{11} . Although the B^{10} targets were free from serious impurities, considerable effort was necessary to produce suitable B^{11} targets. In addition to the usual fluorine contamination on the backing material, the first boron used contained an impurity, probably aluminum, which gave rise to a number of narrow resonances yielding high-energy γ rays and a rather intense low-energy γ ray of about 1 Mev. Targets made from natural boron of greater than 99% purity⁷ were finally used for the γ -ray work and were quite satisfactory.

⁶ Herb, Snowden, and Sala, Phys. Rev. **75**, 246 (1949).

* Elemental B^{10} was obtained from the Stable Isotopes Division of this Laboratory.

⁷ Varlocoid Chemical Company, 116 Broad Street, New York City.